

Electronic structure and metal-insulator transition in $\text{LaNiO}_{3-\delta}$

M. Abbate,¹ G. Zampieri,² F. Prado,² A. Caneiro,² J. M. Gonzalez-Calbet,³ and M. Vallet-Regi⁴

¹*Departamento de Física, Universidade Federal de Paraná, Caixa Postal 19091, 81531-990 Curitiba PR, Brazil*

²*Centro Atómico Bariloche, Comisión Nacional de Energía Atómica, 8400 Bariloche, Rio Negro, Argentina*

³*Facultad de Química, Universidad Complutense, 28040, Madrid, Spain*

⁴*Facultad de Farmacia, Universidad Complutense, 28040, Madrid, Spain*

(Received 11 September 2001; published 18 March 2002)

We studied the changes in the electronic structure of $\text{LaNiO}_{3-\delta}$ across the metal-insulator transition. The technique used in the study was mainly O 1s x-ray absorption spectroscopy (XAS). The experimental spectrum of $\text{LaNiO}_{3.00}$ was analyzed in terms of a cluster-model calculation. The spectrum of $\text{LaNiO}_{3.00}$ presents a sharp peak at a threshold that corresponds to $3d^8L \rightarrow \zeta 3d^9$ transitions. Analysis of this peak indicates that the charge carriers in $\text{LaNiO}_{3.00}$ contain considerable oxygen character. The intensity of this peak decreases in the spectrum of $\text{LaNiO}_{2.75}$ and disappears almost completely for $\text{LaNiO}_{2.50}$. This suggests that the metal-insulator transition is related to the disappearance of the charge carriers and the ensuing band-gap opening. The peak in the $\text{LaNiO}_{2.75}$ compound is split due to the presence of two nonequivalent crystallographic sites. The metal-insulator transition in this compound is tentatively attributed to potential disorder between these two sites.

DOI: 10.1103/PhysRevB.65.155101

PACS number(s): 78.70.Dm, 71.30.+h

I. INTRODUCTION

The nickelates of general formula $R\text{NiO}_3$ (R =rare earth) present very interesting changes in their physical properties.¹⁻³ For instance, LaNiO_3 is metallic at all temperatures, but the other $R\text{NiO}_3$ compounds present a metal-insulator transition. The transition temperature T_{M-I} is related to crystallographic changes associated with differences in the ionic radii of R . In addition, whereas LaNiO_3 is paramagnetic, the other $R\text{NiO}_3$ compounds present antiferromagnetic ordering ($s=1/2$). The transition temperature T_{M-I} coincides with the ordering temperature T_N for the PrNiO_3 and NdNiO_3 compounds. On the other hand, the onset of magnetic ordering for the remaining rare-earth compounds takes place at lower temperatures.

This rich variety of physical properties derives from the interplay of structural, electronic, and magnetic degrees of freedom. Despite many studies, the electronic structure and the metal-insulator transition in $R\text{NiO}_3$ compounds remain still controversial.⁴ Medarde *et al.* proposed a highly covalent $3d^7$ ground state and a transition due to a charge-transfer gap opening.⁵ Barman *et al.* suggested that the origin of the metal-insulator transition was a change in the Ni $3d$ -O $2p$ covalency.⁶ Mizokawa *et al.* indicated that the band gap was not entirely of the p - d type but rather of strongly hybridized pd - pd character.⁷ The metal-insulator transitions considered in all these studies were concerned only with stoichiometric compounds.

Alternatively, a metal-insulator transition can be induced in the $\text{LaNiO}_{3-\delta}$ compound controlling the oxygen concentration. $\text{LaNiO}_{3.00}$ has trivalent Ni^{3+} , is metallic ($\partial\sigma/\partial T < 0$), and exhibits Pauli paramagnetism, whereas $\text{LaNiO}_{2.50}$ has divalent Ni^{2+} , is insulating ($\partial\sigma/\partial T > 0$), and is antiferromagnetic with $T_N=320$ K.⁸ $\text{LaNiO}_{2.75}$ is a mixed-valence system ($\text{Ni}^{3+}/\text{Ni}^{2+}$) and presents a subtle metal-insulator transition around 75 K, as well as spin localization and magnetic frustration.⁸ The Ni ions in $\text{LaNiO}_{3.00}$ occupy only oc-

tahedral sites, whereas in $\text{LaNiO}_{2.50}$ they equally occupy octahedral and square planar sites. Finally, the occupation of the Ni ions in $\text{LaNiO}_{2.75}$ is 66.6% in octahedral sites and 33.3% in square planar sites.

The electronic structure and metal-insulator transition in $\text{LaNiO}_{3-\delta}$ are not completely understood yet. This provides the motivation to study the electronic structure of $\text{LaNiO}_{3-\delta}$ as a function of δ . The experimental technique used in this study was O 1s x-ray absorption spectroscopy (XAS). This technique provides useful information on the unoccupied electronic states in the conduction band.⁹ XAS is also a very sensitive probe of the covalent mixing between the metal $3d$ and oxygen $2p$ levels.¹⁰ The potential of O 1s XAS was demonstrated in several studies of metal-insulator transitions induced by temperature^{11,12} as well as substitution.^{13,14}

II. EXPERIMENTAL DETAILS

The samples studied here were $\text{LaNiO}_{3.00}$, $\text{LaNiO}_{2.75}$, and $\text{LaNiO}_{2.50}$. The reference LaNiO_3 sample was prepared using a liquid mix method.⁸ The other samples were obtained by the reduction of LaNiO_3 in a thermobalance. The flowing H_2/Ar ratio was 0.2 and the temperature was 300 °C. The samples were then annealed in Ar at 400 °C to improve the homogeneity. X-ray diffraction studies confirmed that all samples were single phase. The characterization also included conductivity and susceptibility measurements. Further details on the preparation and characterization can be found in Ref. 8.

The XAS measurements were carried out at the spherical-grating-monochromator (SGM) beamline in the LNLS. The base pressure in the experimental chamber was in the low 10^{-9} -mbar range. The samples were scraped *in situ* with a diamond file to remove surface contamination. The O 1s x-ray absorption spectra were measured using the total electron yield (TEY) method. The probing depth of XAS using the TEY method is approximately 5 nm.¹⁵ The energy scale was calibrated using the known peak positions in LaNiO_3 .⁵

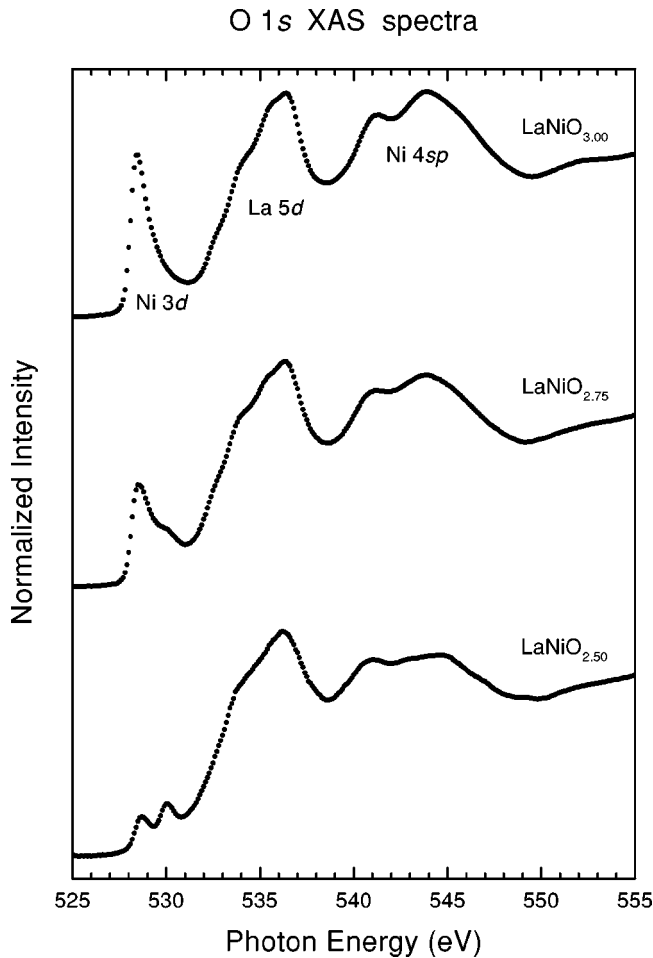


FIG. 1. O $1s$ x-ray absorption spectra of $\text{LaNiO}_{3.00}$, $\text{LaNiO}_{2.75}$, and $\text{LaNiO}_{2.50}$.

The energy resolution at the O $1s$ x-ray absorption edge (around 528.5 eV) was approximately 0.5 eV. The spectra were normalized to the maximum after a constant background subtraction.

The Mn $2p$ x-ray photoelectron spectroscopy (XPS) measurements were performed in a commercial VG equipment. The base pressure in the experimental chamber was in the low- 10^{-10} -mbar range. The samples were scraped with a diamond file before their insertion into the main experimental chamber. The spectra were taken using Al $K\alpha$ photons ($h\nu = 1486.6$ eV) and an electrostatic energy analyzer. The overall energy resolution of the system (photons + analyzer) was approximately 1.0 eV. Survey XPS spectra confirmed the quality of the samples with only a small C residual contamination. The spectra were corrected for the Al $K\alpha_{3,4}$ ghost lines. The spectra were normalized to the maximum after a constant background subtraction.

III. RESULTS AND DISCUSSION

A. O $1s$ XAS spectra of $\text{LaNiO}_{3-\delta}$

Figure 1 shows the O $1s$ x-ray absorption spectra of $\text{LaNiO}_{3.00}$, $\text{LaNiO}_{2.75}$, and $\text{LaNiO}_{2.50}$. First, we note that the spectrum of LaNiO_3 is in excellent agreement with previous

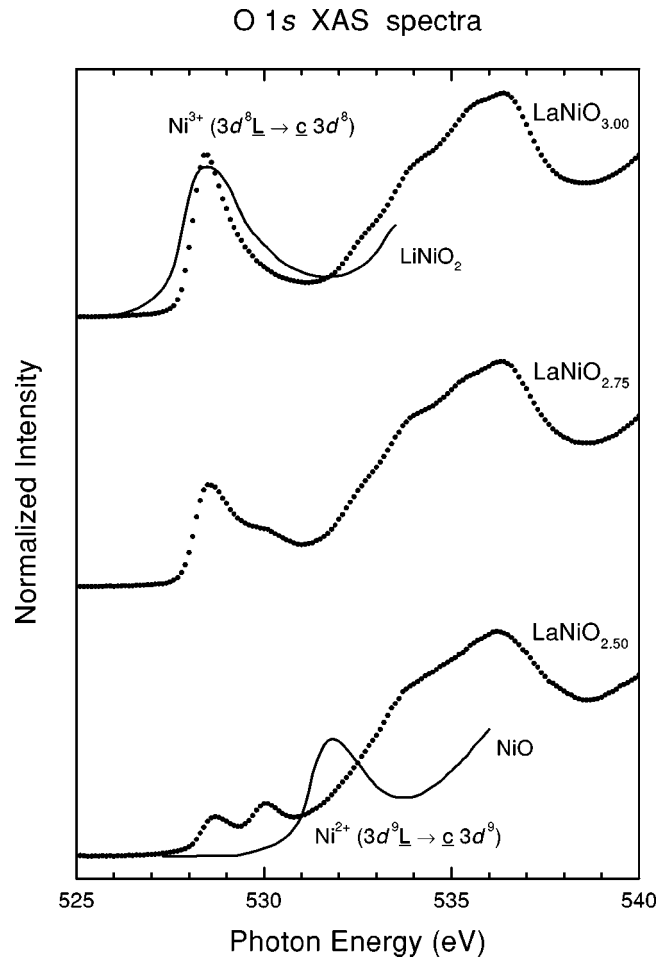


FIG. 2. Ni $3d$ region of the O $1s$ XAS spectra of $\text{LaNiO}_{3.00}$, $\text{LaNiO}_{2.75}$, and $\text{LaNiO}_{2.50}$ (dots) compared to LiNiO_2 and NiO (solid line).

reports.⁵ This spectrum corresponds to transitions to unoccupied O p states in the conduction band. These states reflect, through the oxygen-metal hybridization, bands of mostly metal character.¹⁰ The first peak around 528.5 eV corresponds to the Ni $3d$ band region, the broad structure around 535 eV corresponds to the La $5d$ band region, and the two bumps around 540–545 eV correspond to the Ni $4sp$ band region. These assignments are consistent with previous analysis of the LaMnO_3 , LaFeO_3 , and LaCoO_3 spectra.^{16,17} The spectra of the nonstoichiometric compounds $\text{LaNiO}_{2.75}$ and $\text{LaNiO}_{2.50}$ exhibit several changes. The most relevant change concerns the lowest-lying states in the Ni $3d$ band region.

B. Comparison with $\text{Li}_{1-x}\text{Ni}_x\text{O}$

Figure 2 shows in more detail the Ni $3d$ band region of $\text{LaNiO}_{3.00}$, $\text{LaNiO}_{2.75}$, and $\text{LaNiO}_{2.50}$ (dots). These spectra are compared to the Ni $3d$ band region of the LiNiO_2 and NiO compounds from Ref. 18 (solid line). The Ni ions in the $\text{LaNiO}_{3.00}$ compound are formally in a trivalent Ni^{3+} ($3d^7$) state. The ground state of this compound is composed mainly of $3d^7$ and $3d^8\bar{L}$ configurations, where \bar{L} denotes a ligand

hole. The main peak in $\text{LaNiO}_{3.00}$, around 528.5 eV, corresponds to $3d^8\bar{L} \rightarrow \bar{c}3d^8$ (Ni^{3+}) transitions, where \bar{c} denotes an O 1s core hole. This absorption peak is in excellent concordance with that of the LiNiO_2 compound, which has also trivalent Ni^{3+} ions.¹⁸ This peak decreases in the $\text{LaNiO}_{2.75}$ compound and almost disappears in the $\text{LaNiO}_{2.50}$ compound. The residual intensity in the spectrum of $\text{LaNiO}_{2.50}$ is attributed to a slight oxygen excess. Following Kuiper *et al.*, we estimate that the actual stoichiometry of this sample is approximately $\text{LaNiO}_{2.57}$.¹⁹

The Ni ions in the $\text{LaNiO}_{2.50}$ compound are in a formally divalent Ni^{2+} ($3d^8$) state. The main contribution to the ground state, in this case, is given by the $3d^8$ and $3d^9\bar{L}$ configurations. The main absorption channel in the $\text{LaNiO}_{2.50}$ compound corresponds to $3d^9\bar{L} \rightarrow \bar{c}3d^9$ (Ni^{2+}) transitions. These transitions produce the main peak around 531.7 eV in the spectrum of NiO ,¹⁸ which has also divalent Ni^{2+} ions. The transitions in $\text{LaNiO}_{2.50}$ appear at higher energies and are masked by the stronger La 5d band region. Finally, the Ni ions in the $\text{LaNiO}_{2.75}$ compound are in a mixture of trivalent Ni^{3+} and divalent Ni^{2+} states. The Ni 3d band region, in this case, resembles approximately a linear combination of the parent compounds. The first peak shoulder correspond to Ni^{3+} transitions, whereas the Ni^{2+} transitions are again hidden in the La 5d band region. The splitting of the Ni^{3+} transitions in the $\text{LaNiO}_{2.75}$ compound is related to the two nonequivalent sites; see below.

C. Comparison with $\text{La}_{2-x}\text{Sr}_x\text{NiO}_4$

Figure 3 compares the Ni 3d band region of $\text{LaNiO}_{3.00}$, $\text{LaNiO}_{2.75}$, and $\text{LaNiO}_{2.50}$ (dots) to the spectra of La_2NiO_4 and $\text{La}_{1.2}\text{Sr}_{0.8}\text{NiO}_4$ taken from Ref. 19 (solid line). The main features in the La_2NiO_4 spectrum, which has also divalent Ni^{2+} ions, are rather similar to that of $\text{LaNiO}_{2.50}$. The $3d^9\bar{L} \rightarrow \bar{c}3d^9$ (Ni^{2+}) transitions in the La_2NiO_4 compound are hidden by the stronger La 5d band region.¹⁹ The residual absorption intensity around 529.5 eV in La_2NiO_4 was attributed to a slight oxygen excess.¹⁹ The interpretation of the $\text{LaNiO}_{2.50}$ spectrum is thus consistent with the previous analysis of the La_2NiO_4 spectrum.¹⁹ The substitution of trivalent La^{3+} by divalent Sr^{2+} introduces doped holes in the mixed-valence $\text{La}_{1.2}\text{Sr}_{0.8}\text{NiO}_4$ compound. The $3d^8\bar{L} \rightarrow \bar{c}3d^8$ (Ni^{3+}) transitions in the $\text{La}_{1.2}\text{Sr}_{0.8}\text{NiO}_4$ spectrum are rather similar to those in the $\text{LaNiO}_{2.75}$ compound. The $3d^9\bar{L} \rightarrow \bar{c}3d^9$ (Ni^{2+}) transitions in both compounds are again hidden by the relatively stronger La 5d band region.

D. Nonequivalent site splitting

The Ni^{3+} transitions in the $\text{LaNiO}_{2.75}$ compound are split into a main peak at 528.5 eV and a shoulder around 530.0 eV. This splitting can be understood taking into account the presence of the two nonequivalent sites in this compound.⁸ The main peak coincides with the peak in the spectrum of $\text{LaNiO}_{3.00}$ and is thus ascribed to Ni^{3+} ions in octahedral (O_h) symmetry. On the other hand, the shoulder at higher energies is attributed to Ni^{3+} ions occupying square planar (D_{4h}) sites, as indicated in Fig. 3. This interpretation is sup-

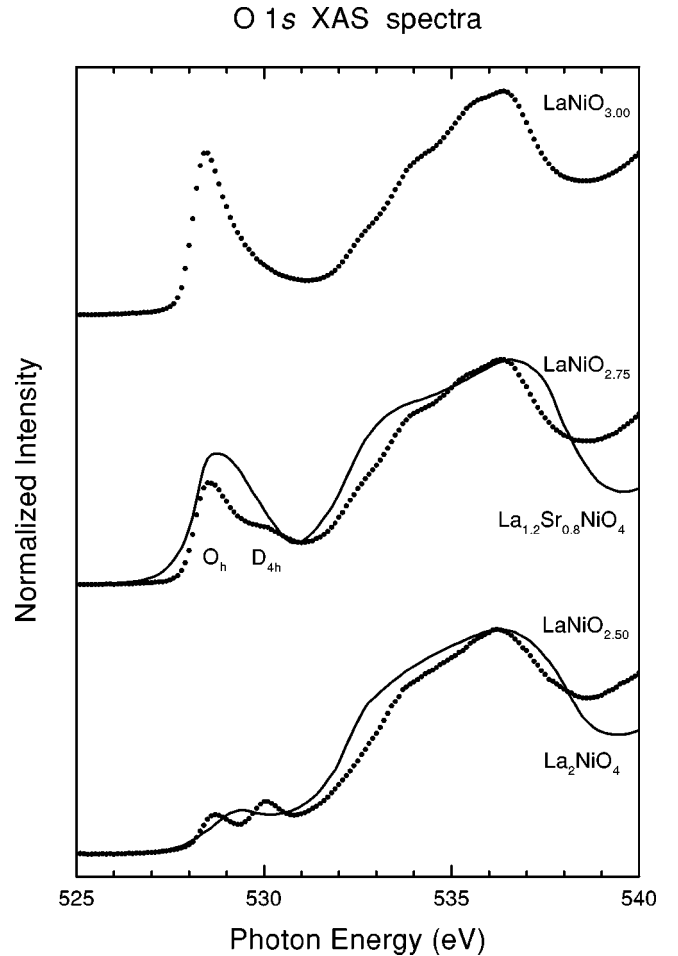


FIG. 3. Ni 3d region of the O 1s XAS spectra of $\text{LaNiO}_{3.00}$, $\text{LaNiO}_{2.75}$, and $\text{LaNiO}_{2.50}$ (dots) compared to $\text{La}_{1.2}\text{Sr}_{0.8}\text{NiO}_4$ and La_2NiO_4 (solid line).

ported by the intensity ratio between the main peak and shoulder, approximately 2:1; which is in perfect agreement with the ratio of octahedral to square planar sites in the $\text{LaNiO}_{2.75}$ compound.⁸ Further support to these assignments is given by the 1:1 intensity ratio of the residual Ni^{3+} peaks in $\text{LaNiO}_{2.50}$, which has equally populated O_h and D_{4h} sites.⁸ The splitting of the Ni^{2+} transitions in the $\text{LaNiO}_{2.75}$ and $\text{LaNiO}_{2.50}$ compounds is masked by the stronger La 5d band region.

The higher energy of the Ni^{3+} transitions in D_{4h} symmetry can be related to changes in the charge-transfer energy Δ . The lower coordination in the square planar sites leads to a smaller Madelung stabilization of the Ni^{3+} ions. In turn, the reduced energy of the Ni 3d level compared to the O 2p level results in an increase in the charge-transfer energy Δ . Finally, the larger value of the charge-transfer energy Δ pushes up the first affinity state, giving higher-energy Ni^{3+} transitions. The same argument could be applied to the charge-transfer energy Δ corresponding to the Ni^{2+} ions occupying square planar sites. This means that the Ni^{2+} transitions in D_{4h} symmetry should, in principle, occur at higher energies than in O_h symmetry. This might help to explain

why the Ni^{2+} transitions in both La_2NiO_4 and $\text{LaNiO}_{2.50}$ appear at higher energies than in NiO . Unfortunately, the details of the Ni^{2+} transitions in these compounds are masked by the overlap with the stronger La $5d$ band region.

E. Metal-insulator transition

The metallic conduction in $\text{LaNiO}_{3.00}$ is related to charge fluctuations involving the lowest-lying Ni^{3+} derived states. But the Ni^{3+} ions are continuously transformed into Ni^{2+} ions as the oxygen content of the compound is decreased. Accordingly, the Ni^{3+} -derived states decrease in $\text{LaNiO}_{2.75}$ and disappear almost completely in the $\text{LaNiO}_{2.50}$ compound. The next available states in $\text{LaNiO}_{2.50}$ correspond to the Ni^{2+} -derived states which appear at considerably higher energies. The insulating character of $\text{LaNiO}_{2.50}$ is thus attributed to the disappearance of the Ni^{3+} -derived states and the ensuing band-gap opening. The overlap of the Ni^{2+} transitions and the La $5d$ band region precludes a precise determination of the band gap, but using the Fermi level from $\text{LaNiO}_{3.00}$ and the tail of the La $5d$ band from $\text{LaNiO}_{2.50}$ the band gap should be at least 5 eV. The larger value of the band gap in $\text{LaNiO}_{2.50}$ compared to NiO can be traced back to the larger charge-transfer energy Δ ; see below.

The $\text{LaNiO}_{2.75}$ compound represents an intermediate situation between the $\text{LaNiO}_{3.00}$ and $\text{LaNiO}_{2.50}$ compounds. The intensity of the Ni^{3+} transitions in this compound is considerable and there is no shift of the edge or peak positions. At first sight, this would suggest a metallic character for $\text{LaNiO}_{2.75}$ which is at variance with the observed electrical conductivity. This compound presents a relatively temperature-independent conductivity ($\partial\sigma/\partial T \approx 0$) and a subtle metal-insulator transition around 75 K.⁸ This apparent discrepancy could be reconciled assuming that the Ni^{3+} -derived states become localized in the $\text{LaNiO}_{2.75}$ compound. Following Sanchez *et al.*, the localization is tentatively attributed to potential disorder caused by the presence of the oxygen vacancies.⁸ This interpretation is here supported by the large energy difference observed between the Ni^{3+} ions in octahedral and square planar sites. Additional evidence comes from the relatively high sensitivity of the electrical conductivity on the annealing conditions of the $\text{LaNiO}_{2.75}$ compound.⁸

F. Ni $2p$ XPS spectra

Figure 4 shows the Ni $2p_{1/2}$ peak region of the x-ray photoelectron spectra of $\text{LaNiO}_{3.00}$ and $\text{LaNiO}_{2.50}$ (the Ni $2p_{3/2}$ peak is not shown because it overlaps with the La $3d_{3/2}$ peak). The spectra present a main Ni $2p_{1/2}$ peak around 876.5 eV and a relatively broad satellite about 885.5 eV. The main peak corresponds to the so-called *well-screened* final-state configuration $\bar{c}3d^{n+1}L$, whereas the satellite corresponds to the so-called *poorly screened* final-state configuration $\bar{c}3d^n$ (where \bar{c} denotes a core hole in the Ni $2p$ level). The Ni $2p_{1/2}$ XPS spectra were analyzed using the well-known configuration interaction approach. The main parameters of the calculation are the core-hole potential Q , the Mott-Hubbard repulsion U , the charge-transfer energy Δ ,

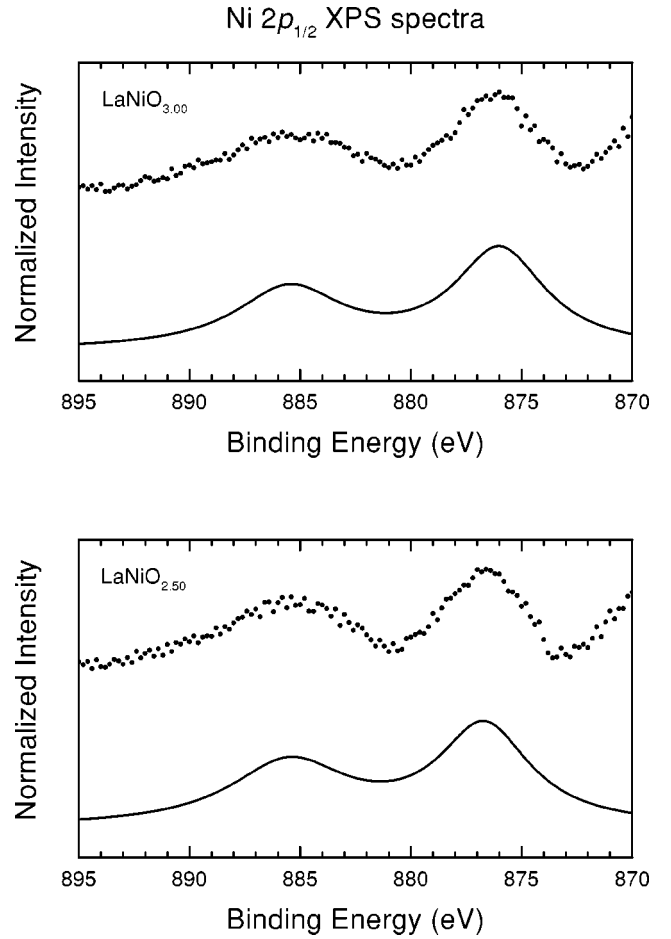


FIG. 4. Ni $2p_{1/2}$ X-ray photoelectron spectra of $\text{LaNiO}_{3.00}$ and $\text{LaNiO}_{2.50}$ (dots) compared to the configuration interaction calculation (solid line).

and the transfer integral ($pd\sigma$) (it is assumed that the core-hole potential Q and the Mott-Hubbard repulsion U are linked by the relation $U \approx 0.8Q$).

Figure 4 compares the calculated (solid line) and the experimental (dots) spectra of $\text{LaNiO}_{3.00}$ and $\text{LaNiO}_{2.50}$. Good agreement with the $\text{LaNiO}_{3.00}$ spectrum is obtained for $Q = 9.0$ eV, $U = 7.0$ eV, $\Delta = 1.0$ eV, and $(pd\sigma) = 1.8$ eV. The multiplet splitting and crystal field parameters were set to $B = 0.14$ eV, $C = 0.53$ eV, and $10Dq = 1.0$ eV. This parameter set is in very good agreement with that of the related PrNiO_3 compound.⁷ This gives a highly covalent low-spin 2E ground state with 28% $3d^7$, 60% $3d^8\bar{L}$, 10% $3d^9\bar{L}^2$, and 2% $3d^{10}\bar{L}^3$ (the high-spin 4T_1 state appears at higher energies, as in the PrNiO_3 compound).⁷ It is worth noting that the occupation of the $3d^8\bar{L}$ configuration is larger than that of the $3d^7$ configuration. The $3d^8\bar{L}$ ground-state configuration appears actually at a lower energy due to multiplet effects (this means that the effective charge-transfer energy Δ_{eff} is negative).^{20,21} Finally, the charge fluctuations in the $\text{LaNiO}_{3.00}$ compound are of strongly mixed pd - pd character, as in the PrNiO_3 case.⁷

Good agreement with the $\text{LaNiO}_{2.50}$ spectrum is obtained for $Q = 10.0$ eV, $U = 8.0$ eV, $\Delta = 6.0$ eV, and $(pd\sigma) = 1.5$ eV. The multiplet splitting and crystal field param-

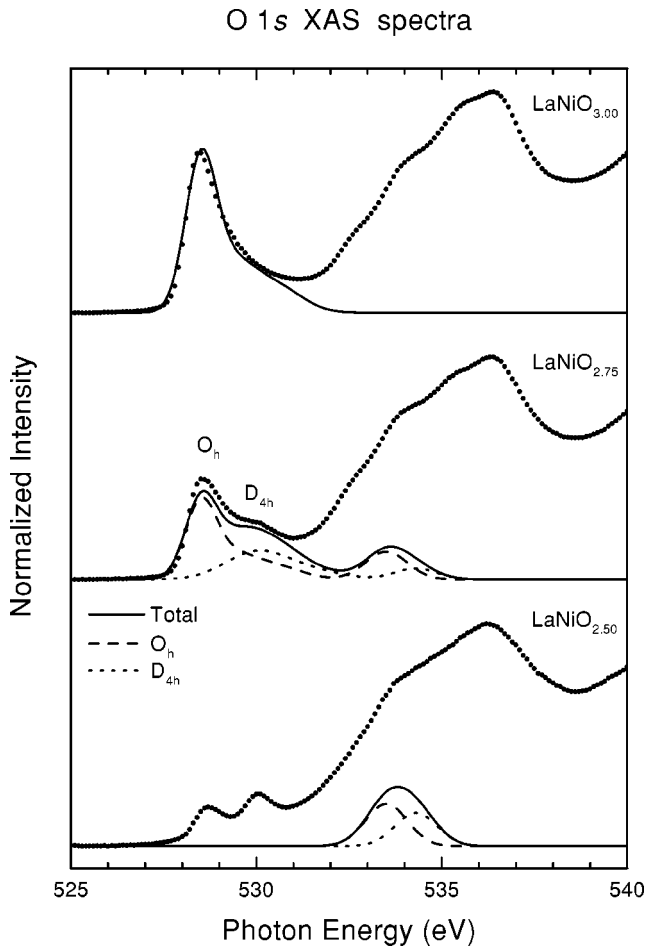


FIG. 5. Ni $3d$ region of the O $1s$ XAS spectra of $\text{LaNiO}_{3.00}$, $\text{LaNiO}_{2.75}$, and $\text{LaNiO}_{2.50}$ (dots) compared to the cluster-model calculation (solid line).

eters were set to $B=0.11$ eV, $C=0.48$ eV, and $10Dq=1.0$ eV. This parameter set is in very good agreement with that of the related La_2NiO_4 compound.¹⁹ The occupation of the configurations in the rather ionic high-spin 3A_2 ground state are 73% $3d^8$, 26% $3d^9L$, and 1% $3d^{10}L^2$. The band gap of $\text{LaNiO}_{2.50}$ is dictated by the charge-transfer energy Δ and involves mainly p - d fluctuations. The charge-transfer energy in the $\text{LaNiO}_{2.50}$ compound, $\Delta=6.0$ eV, is larger than in the NiO compound, $\Delta=4.0$ eV. This produces a larger band gap and explains why the Ni^{2+} transitions in $\text{LaNiO}_{2.50}$ appear at higher energies than in NiO . The same argument concerning the band gap and the Ni^{2+} transitions applies to the related La_2NiO_4 compound.¹⁹

G. Cluster-model calculations

Figure 5 shows the cluster-model calculations of the Ni $3d$ region of the O $1s$ XAS spectra. The method of calculation follows that used in the closely related PrNiO_3 compound.⁷ The relative energy of the transitions is mostly given by the energies of the different $3d^n$ final-state configurations. The relative intensities of the transitions are mainly given by the occupations of the $3d^nL$ terms in the ground state. The absolute energy and intensity of all the calcula-

tions were adjusted so as to match the Ni^{3+} transitions in $\text{LaNiO}_{3.00}$. The model parameters used in the calculation were derived from analysis of the Ni $2p$ XPS spectra. The calculation for the $\text{LaNiO}_{3.00}$ compound included only $3d^8L \rightarrow \epsilon 3d^8$ (Ni^{3+}) transitions in O_h symmetry. The result for $\text{LaNiO}_{3.00}$ is similar to that of the related PrNiO_3 compound and is in good agreement with the experiment.⁷ The relatively high intensity of these transitions follows from the large O character mixed in the ground state.

The calculation for the $\text{LaNiO}_{2.50}$ compound included $3d^9L \rightarrow \epsilon 3d^9$ (Ni^{2+}) transitions in O_h and D_{4h} symmetry. The O_h part represents the Ni^{2+} ions in octahedral symmetry and the D_{4h} part the Ni^{2+} ions in square planar symmetry. The model parameters used in the calculation were derived from the analysis of the Ni $2p$ XPS spectra. To simulate the D_{4h} environment, the hybridization with the Ni $3d_{z^2}$ orbital was switched off and the change of the Madelung energy ΔM was set to 1.0 eV; see below. The calculation for $\text{LaNiO}_{2.50}$ presents the O_h and D_{4h} transitions hidden in the La $5d$ region of the spectrum. The energy shift between the O_h and D_{4h} transitions is given by the differences in the hybridization and the Madelung energy. The smaller intensity of the D_{4h} transition is due to the reduced hybridization in the ground state.

The calculation for the $\text{LaNiO}_{2.75}$ compound included Ni^{3+} and Ni^{2+} transitions in O_h and D_{4h} symmetry. The parameters for the Ni^{3+} calculation were taken from $\text{LaNiO}_{3.00}$ and those for the Ni^{2+} calculation from $\text{LaNiO}_{2.50}$. To simulate the D_{4h} environment, the hybridization with the Ni $3d_{z^2}$ orbital was switched off for both Ni^{3+} and Ni^{2+} transitions. In addition, the change of the Madelung energy ΔM was set to 1.5 eV for the Ni^{3+} transitions and 1.0 eV for the Ni^{2+} transitions (the value of ΔM for the Ni^{3+} transitions produces the right energy separation between the O_h and D_{4h} peaks; the value of ΔM for the Ni^{2+} transitions was scaled down according to the corresponding ionic charge). The calculation for $\text{LaNiO}_{2.75}$ reproduces reasonably well all the Ni^{3+} transitions in the experimental spectrum. The main peak at 528.5 eV corresponds to Ni^{3+} transitions in O_h symmetry, whereas the shoulder around 530.0 eV corresponds to Ni^{3+} transitions in D_{4h} symmetry. Unfortunately, as in the $\text{LaNiO}_{2.50}$ compound, the Ni^{2+} transitions in O_h and D_{4h} are completely masked by the stronger La $5d$ band region.

IV. SUMMARY AND CONCLUSIONS

In summary, we studied the changes in the electronic structure of $\text{LaNiO}_{3-\delta}$ across the metal-insulator transition. The technique used in the study was mainly O $1s$ x-ray absorption spectroscopy. The experimental spectrum of $\text{LaNiO}_{3.00}$ was analyzed in terms of a cluster-model calculation. The spectrum of $\text{LaNiO}_{3.00}$ presents a sharp peak at threshold which corresponds to $3d^8L \rightarrow \epsilon 3d^9$ transitions. Analysis of this peak indicates that the charge carriers in $\text{LaNiO}_{3.00}$ contain considerable oxygen character. The intensity of this peak decreases in the spectrum of $\text{LaNiO}_{2.75}$ and disappears almost completely for $\text{LaNiO}_{2.50}$. This suggests

that the metal-insulator transition is related to the disappearance of the charge carriers and the ensuing band-gap opening. The peak in the $\text{LaNiO}_{2.75}$ compound is split due to the presence of two nonequivalent crystallographic sites. The metal-insulator transition in this compound is tentatively attributed to potential disorder between these two sites.

ACKNOWLEDGMENTS

We would like to thank the technical staff of the LNLS for their helpful assistance during the measurements. This work was partially supported by CNPq, PRONEX, LNLS, Fundación Antorchas, and Fundação Araucaria.

-
- ¹P. Lacorre, J.B. Torrance, J. Pannetier, A.I. Nazzal, P.W. Wang, and T.C. Huang, *J. Solid State Chem.* **91**, 225 (1991).
- ²J.B. Torrance, P. Lacorre, A.I. Nazal, E.J. Ansaldo, and C. Niedermayer, *Phys. Rev. B* **45**, 8209 (1992).
- ³J.L. Garcia-Muñoz, J. Rodriguez-Carvajal, P. Lacorre, and J.B. Torrance, *Phys. Rev. B* **46**, 4414 (1992).
- ⁴M.L. Medarde, *J. Phys.: Condens. Matter* **9**, 1679 (1997).
- ⁵M. Medarde, A. Fontaine, J.L. Garcia-Muñoz, J. Rodriguez-Carvajal, M. de Santis, M. Sacchi, G. Rossi, and P. Lacorre, *Phys. Rev. B* **46**, 14 975 (1992).
- ⁶S.R. Barman, A. Chainani, and D.D. Sarma, *Phys. Rev. B* **49**, 8475 (1994).
- ⁷T. Mizokawa, A. Fujimori, T. Arima, Y. Tokura, N. Mori, and J. Akimitsu, *Phys. Rev. B* **52**, 13 865 (1995).
- ⁸R.D. Sanchez, M.T. Causa, C. Caneiro, A. Butera, M. Vallet-Regi, M.J. Sayagues, J. Gonzalez-Calbet, F. Garcia-Sanz, and J. Rivas, *Phys. Rev. B* **54**, 16 574 (1996).
- ⁹J.C. Fuggle and J.E. Inglesfield, *Unoccupied Electronic States* (Springer, Berlin, 1992).
- ¹⁰M. Abbate, H. Pen, M.T. Czyzyk, F.M.F. de Groot, J.C. Fuggle, Y.J. Ma, C.T. Chen, F. Sette, A. Fujimori, Y. Ueda, and K. Kosuge, *J. Electron Spectrosc. Relat. Phenom.* **62**, 185 (1993).
- ¹¹M. Abbate, F.M.F. de Groot, J.C. Fuggle, Y.J. Ma, C.T. Chen, F. Sette, A. Fujimori, Y. Ueda, and K. Kosuge, *Phys. Rev. B* **43**, 7263 (1991).
- ¹²M. Abbate, R. Potze, G.A. Sawatzky, C. Schlenker, H.J. Lin, L.H. Tjeng, C.T. Chen, D. Teehan, and T.S. Turner, *Phys. Rev. B* **51**, 10 150 (1995).
- ¹³A. Fujimori, I. Hase, M. Nakamura, H. Namatame, Y. Fujishima, Y. Tokura, H. Eisaki, S. Uchida, M. Abbate, F.M.F. de Groot, M.T. Czyzyk, J.C. Fuggle, O. Strebel, F. Lopez, M. Domke, and G. Kaindl, *Phys. Rev. B* **46**, 9841 (1992).
- ¹⁴H.F. Pen, M. Abbate, A. Fujimori, Y. Tokura, H. Eisaki, S. Uchida, and G.A. Sawatzky, *Phys. Rev. B* **59**, 7422 (1999).
- ¹⁵M. Abbate, J.B. Goedkoop, F.M.F. de Groot, M. Grioni, J.C. Fuggle, S. Hofmann, H. Petersen, and M. Sacchi, *Surf. Interface Anal.* **18**, 65 (1992).
- ¹⁶M. Abbate, F.M.F. de Groot, J.C. Fuggle, A. Fujimori, O. Strebel, F. Lopez, M. Domke, G. Kaindl, G.A. Sawatzky, M. Takano, Y. Takeda, H. Eisaki, and S. Uchida, *Phys. Rev. B* **46**, 4511 (1992).
- ¹⁷M. Abbate, J.C. Fuggle, A. Fujimori, L.H. Tjeng, C.T. Chen, R. Potze, G.A. Sawatzky, H. Eisaki, and S. Uchida, *Phys. Rev. B* **47**, 16 124 (1993).
- ¹⁸P. Kuiper, G. Kruizinga, J. Ghijsen, G.A. Sawatzky, and H. Verweij, *Phys. Rev. Lett.* **62**, 221 (1989).
- ¹⁹P. Kuiper, J. van Elp, G.A. Sawatzky, A. Fujimori, S. Hosoya, and D.M. de Leeuw, *Phys. Rev. B* **44**, 4570 (1991).
- ²⁰J. Zaanen, G.A. Sawatzky, and J.W. Allen, *Phys. Rev. Lett.* **55**, 418 (1985).
- ²¹T. Mizokawa, H. Namatame, A. Fujimori, K. Akeyama, H. Kondoh, H. Kuroda, and N. Kosigi, *Phys. Rev. Lett.* **67**, 1638 (1991).